phenylhydroquinone, illustrates the difference between minisegmented and fully aromatic poly(ether ketone)s. Of course, the thermogravimetric analyses presented in Table IV and Figure 9 only give information on the short-time thermostability which defines the upper limit for any thermal processing. The long-term stability of minisegmented poly(ester ketone)s will certainly be significantly lower than that of fully aromatic polymers.

Acknowledgment. We thank Dr. G. Scholtyssek and Prof. Dr. H. G. Zachmann (University of Hamburg) for the ^{1}H NMR broad-line measurements.

Registry No. **2a** (copolymer), 116701-89-4; **2a** (SRU), 116701-72-5; **2b** (copolymer), 116701-90-7; **2b** (SRU), 116701-73-6; **2c** (copolymer), 116701-91-8; **2c** (SRU), 116701-74-7; **2d** (copolymer), 116701-93-0; **2d** (SRU), 116701-75-8; **3a** (copolymer), 116701-96-3; **3a** (SRU), 116701-77-0; **3b** (copolymer), 116724-89-1; **3b** (SRU), 116701-78-1; **3c** (copolymer), 116701-97-4; **3c** (SRU), 116701-79-2; **3d** (copolymer), 116701-98-5; **3d** (SRU), 116701-80-5; **4a** (copolymer), 116702-01-3; **4a** (SRU), 116724-88-0; **4b** (copolymer), 116702-02-4; **4b** (SRU), 116701-82-7; **4c** (copolymer), 116702-03-5; **4c** (SRU), 116701-83-8; **4d** (copolymer), 116702-04-6; **4d** (SRU), 116701-84-9; **5a** (copolymer), 116701-94-1; **5a** (SRU), 116701-76-9; **5b** (copolymer), 116701-99-6; **5b** (SRU), 116701-81-6; **6c**, 116702-00-2; **7b**, 95042-14-1; **7d**, 116701-92-9; **9c**, 116724-85-7; **10c**, 115914-44-8; **13**, 116724-87-9; **14**, 116724-86-8; diphenyl tetradecanedicarboxylate, 116724-84-6; tetradecanedicarboxyl chloride, 21646-49-1; hexamethyldisilazane, 999-97-3; phenol, 108-95-2; bis(4-(4-phenoxybenzoyl)phenyl) ether, 63347-89-7; 4-fluorobenzoyl chloride, 403-43-0.

References and Notes

(1) Attwood, T. E.; Barr, D. A.; King, T.; Newton, A. B.; Rose, J. B. *Polymer* **1977**, *18*, 359.
(2) Attwood, T. E.; Dawson, P. C.; Freeman, J. L.; Hoy, L. R. J.; Rose, J. B.; Staniland, P. A. *Polymer* **1981**, *22*, 1096.
(3) Dawson, P. C.; Blundell, D. J. *Polymer* **1980**, *21*, 577.
(4) Kricheldorf, H. R.; Bier, G. *Polymer* **1984**, *25*, 1151.
(5) Kricheldorf, H. R.; Delius, U. *New Polym. Mater.* **1988**, *1*, 127.
(6) Treibs, W.; Falk, F. *Chem. Ber.* **1954**, *87*, 345.
(7) Varma, J. P.; Aggarwal, J. S. *J. Indian Chem. Soc.* **1959**, *36*, 41.
(8) Wagner, R. DOS 3527862, Aug 2, 1985, to Bayer AG.
(9) Al-Dujaili, A. H.; Jenkins, A. D.; Walton, D. R. M. *Makromol. Chem., Rapid Commun.* **1984**, *5*, 33.
(10) Lovinger, A.; Davis, D. D. *Macromolecules* **1986**, *19*, 1861.
(11) Noel, C.; Friedric, C.; Bosio, L.; Strazielle, C. *Polymer* **1984**, *25*, 1281.
(12) Frosini, V.; Marchetti, A.; De Petris, S. *Makromol. Chem., Rapid Commun.* **1982**, *3*, 795.
(13) Kricheldorf, H. R.; Pakull, R. *Macromolecules* **1988**, *21*, 551.
(14) Kricheldorf, H. R.; Pakull, R. *Polymer* **1987**, *28*, 1772.
(15) Pfeifer, H. In *NMR—Basic Principles and Progress*; Diehl, P., Fluck, E., Kosfeld, R., Eds.; Springer-Verlag: Berlin-Heidelberg-New York, 1972; Vol. 7, p 53.
(16) Scholtyssek, G.; Zachmann, H. G.; Kricheldorf, H. R., manuscript in preparation.

Liquid Crystalline Polyethers Based on Conformational Isomerism. 2. Thermotropic Polyethers and Copolyethers Based on 1-(4-Hydroxyphenyl)-2-(2-methyl-4-hydroxyphenyl)ethane and Flexible Spacers Containing an Odd Number of Methylene Units

Virgil Percec* and Raymond Yourd

Department of Macromolecular Science, Case Western Reserve University, Cleveland, Ohio 44106. *Received April 21, 1988*

ABSTRACT: The synthesis and characterization of the first examples of thermotropic main-chain liquid crystalline polyethers and copolyethers based on flexible rodlike mesogenic units or rodlike mesogenic units based on conformational isomerism and flexible spacers are described. The particular examples presented in this paper refer to polyethers (MBPE-5, MBPE-7, MBPE-9, and MBPE-11) and copolyethers (MBPE-X/Y; X, Y = 5, 7, 9, 11) based on 1-(4-hydroxyphenyl)-2-(2-methyl-4-hydroxyphenyl)ethane (MBPE) and flexible spacers containing 5, 7, 9, and 11 methylene units. Both MBPE-5 and MBPE-9 exhibit a nematic and a smectic monotropic mesophase and MBPE-7 is crystalline, while MBPE-11 displays a monotropic nematic mesophase. Copolymers with various compositions close to a 50/50 molar ratio of the two spacers exhibit both nematic and smectic enantiotropic mesophases. Both liquid crystalline transition temperatures and the corresponding enthalpies of the copolymers are weight-averaged values of the similar parameters of the parent homopolymers. Extrapolation of mesomorphic transition temperatures and of enthalpy changes has demonstrated that all homopolymers exhibit virtual nematic and smectic mesophases. The thermal transition temperatures and the enthalpy changes associated with the virtual nematic and smectic mesomorphic transitions of the homopolymers were determined from several sets of copolymers with very good agreement.

Introduction

Traditional *rigid rodlike* mesogenic units are constituted of linearly substituted aromatic or cycloaliphatic rings connected by rigid interconnecting groups which provide a linear and eventually planar conformation to the resulting compound. Although there is free rotation about certain carbon–carbon single bonds of these compounds, it is essential that rotation about these single bonds does not perturb the elongated or extended conformation of the mesogenic group. Therefore, in *rigid rodlike* mesogenic units, the extended conformation of the molecule is accomplished and maintained through the rigidity and linearity of its constituents, i.e., its rigid rodlike character (Scheme I).

The transplant of this concept from low molar mass liquid crystals to macromolecular liquid crystals led to the presently accepted pathway used in the synthesis of both main-chain and side-chain liquid crystalline polymers.

An alternative solution to the creation of an extended conformation of a molecule can be considered when the rigid interconnecting groups from the *rigid rodlike mesogens* are replaced with *flexible* interconnecting units, as, for example, ethylene or methyleneoxy. Although ethylene and methyleneoxy units can adopt an extended confor-

0024-9297/89/2222-0524$01.50/0

Scheme I
Comparison of Rigid and Flexible Rodlike Mesogens or Rodlike Mesogens Based on Conformational Isomerism

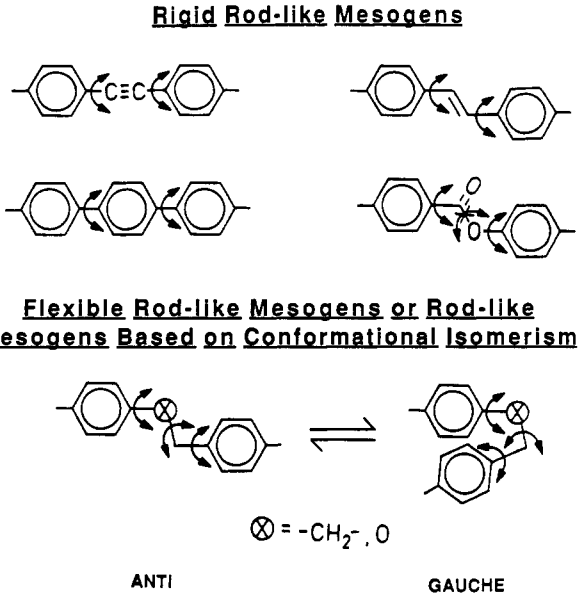

mation which is similar to the trans one provided by an ester or trans-1,2-disubstituted vinylene units (Scheme I), these flexible interconnecting groups undergo free rotation leading to a number of different conformational isomers which are in dynamic equilibrium. Usually the two most stable conformational isomers are anti and gauche (Scheme I). Since the anti conformer has an extended conformation, it is expected to display liquid crystallinity. The gauche conformer is similar to a "kinked" unit which is occasionally introduced within the structure of main-chain liquid crystalline copolymers to depress phase transition temperatures. The anti and gauche conformers are in dynamic equilibrium. Therefore, the insertion of flexible units capable of giving rise to extended and kinked conformers, as, for example, 1,2-diphenylethane, benzyl ether, and methyleneoxy, within the main chain of the polymer is expected to provide a liquid crystalline polymer having a dynamic composition.

In contrast to mesogenic units where the linearity and planarity of the molecule are realized and maintained through their rigid rodlike character, in the second class of mesogens the rodlike character is realized through the conformational isomerism and maintained through the dynamic equilibrium between different conformers. Therefore, for this second class of liquid crystals or mesogenic groups, we have suggested the name *liquid crystals or rodlike mesogenic units based on conformational isomerism.*[1]

The literature on low molar mass "flexible" liquid crystals was briefly mentioned in the previous paper from this series[1] and in more detail in a recent review.[2] The first examples of liquid crystal polymers containing *rodlike mesogenic units based on conformational isomerism* belong to the class of thermotropic side-chain liquid crystalline polymers and were recently reported from our laboratory.[3-5] The first examples of thermotropic quasi-rigid polyethers (i.e., polyethers without flexible spacers) based on conformational isomerism were described in the previous paper from this series.[1]

The goal of this paper is to introduce the conformational isomerism-based liquid crystallinity concept to the synthesis of thermotropic main-chain liquid crystalline polyethers and copolyethers containing flexible spacers. In this case the rodlike character of the mesogenic unit is realized

Scheme II
Synthesis of 1-(4-Hydroxyphenyl)-2-(2-methyl-4-hydroxyphenyl)ethane (MBPE)

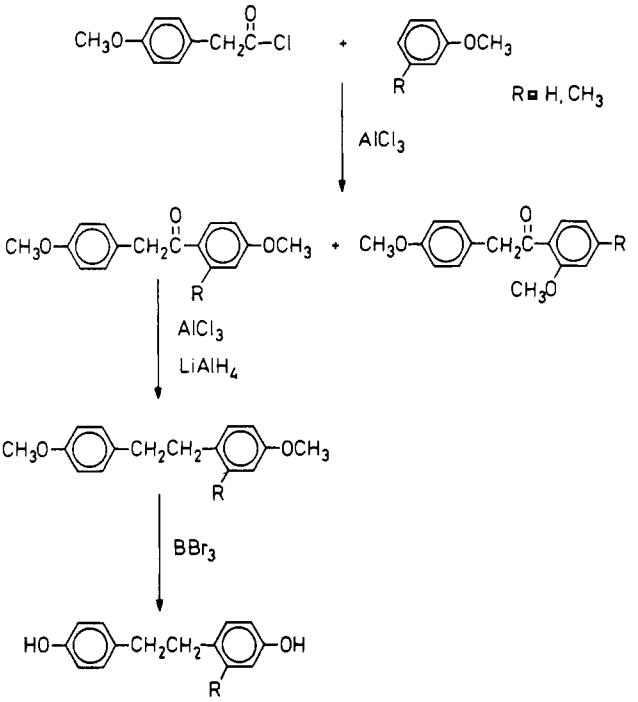

through the conformational isomerism of the flexible mesogenic unit. The examples described here are based on 1-(4-hydroxyphenyl)-2-(2-methyl-4-hydroxyphenyl)-ethane (MBPE) as the flexible rodlike mesogenic unit or a rodlike mesogenic unit based on conformational isomerism and flexible spacers containing 5, 7, 9, and 11 methylene units.

Experimental Section

Materials. Boron tribromide (1.0 M in CH_2Cl_2), 1,5-dibromopentane (97%), 1,7-dibromoheptane (97%), 1,9-dibromononane (97%), 1,11-dibromoundecane (98%), lithium aluminum hydride (99%), thionyl chloride (97%), dimethyl sulfate (99%), tetrabutylammonium hydrogen sulfate (TBAH) (97%), *o*-dichlorobenzene (99%) (all from Aldrich), 4-methoxyphenylacetic acid (99%, Lancaster Synthesis) and *m*-cresol (96.5%, Kodak) were used as received.

Chloroform and methylene chloride were dried over calcium hydride followed by distillation. Diethyl ether was dried over $LiAlH_4$ and then distilled.

Scheme II outlines the synthesis of 1-(4-hydroxyphenyl)-2-(2-methyl-4-hydroxyphenyl)ethane.

Synthesis of 3-Methylanisole. *m*-Cresol (54.0 g, 0.50 mol) was added to a solution of NaOH (21.0 g, 0.50 mol) in 200 mL of H_2O. The mixture was chilled to 10 °C in an ice–water bath and 63.1 g (0.50 mol) of dimethyl sulfate was added dropwise. The reaction mixture was heated at 60 °C for 4 h after which the organic layer was diluted with diethyl ether and separated. The aqueous layer was washed with diethyl ether and the combined ether layers were washed sequentially with H_2O, 5% NaOH, H_2O, dilute HCl, and H_2O. The ether layer was dried over anhydrous magnesium sulfate and the ether was removed in a rotary evaporator. The remaining product was distilled at 175 °C to give 37.2 (60.9%) of a liquid of 99.9% purity (GC). ^1H NMR ($CDCl_3$, TMS, δ, ppm) 2.32 (3 protons, CH_3, s), 3.75 (3 protons, OCH_3, s), 6.72 (3 protons, ortho and para to methoxy, t), 7.16 (1 proton, meta to methoxy, t).

Synthesis of 1-(2-Methyl-4-methoxyphenyl)-2-(4-methoxyphenyl)ethanone. Thionyl chloride (45.67 g, 0.384 mol) was added dropwise to a mixture of 42.53 g (0.256 mol) of 4-methoxyphenylacetic acid and 200 mL of dry methylene chloride. The resulting solution was refluxed for 2 h after which methylene chloride and the excess of thionyl chloride were removed by

distillation under reduced pressure. The resulting acid chloride was used directly in the acylation reaction.

(4-Methoxyphenyl)acetyl chloride (47.25 g, 0.256 mol) and 3-methylanisole (46.9 g, 0.384 mol) were dissolved in 250 mL of dry methylene chloride. The resulting solution was cooled to below 10 °C in an ice–water bath after which 51.2 g (0.383 mol) of anhydrous $AlCl_3$ was added slowly and in small portions so that the reaction temperature did not rise above 15 °C. After all the $AlCl_3$ had been added, the ice bath was removed and the deep red solution was stirred at room temperature for 15 min. The reaction mixture was then poured into a mixture of 100 mL of concentrated HCl and 400 mL of ice–water. The organic layer was separated and washed sequentially with H_2O, 10% aqueous NaOH, and H_2O, after which it was dried over anhydrous $MgSO_4$ and filtered and the methylene chloride was removed in a rotary evaporator. The unreacted 3-methylanisole was removed by distillation at 38 °C (2 mmHg). The golden syrup which contains a mixture of ortho and para isomers was recrystallized from 250 mL of 95% ethanol to give 23.8 g (34.4%) of white needle-like crystals: mp (DSC, 20 °C/min) 80 °C; purity (HPLC) 98.7%; ^{1}H NMR ($CDCl_3$, TMS, δ, ppm) 2.51 (3 protons, CH_3, s), 3.78 (3 protons, OCH_3 of the unsubstituted phenyl ring, s), 3.83 (3 protons, OCH_3 of the methylsubstituted phenyl ring, s), 4.13 (2 protons, CH_2CO, s), 6.74 (2 protons, ortho to methoxy of the substituted phenyl ring, s and d), 6.85 (2 protons, ortho to methoxy of the unsubstituted phenyl ring, d), 7.15 (2 protons, meta to methoxy of the unsubstituted phenyl ring, d), 7.81 (1 proton, meta to methoxy of the substituted phenyl ring, d).

Synthesis of 1-(4-Methoxyphenyl)-2-(2-methyl-4-methoxyphenyl)ethane. It was prepared by the reduction of 1-(2-methyl-4-methoxyphenyl)-2-(4-methoxyphenyl)ethanone with $LiAlH_4/AlCl_3$[6,7] as follows. $AlCl_3$ (31.0 g, 0.232 mol) was slowly added to 200 mL of dry diethyl ether and the resulting solution was added dropwise from an addition funnel to a slurry of $LiAlH_4$ (4.1 g, 0.105 mol) in 80 mL of a dry diethyl ether under nitrogen atmosphere. To this reducing agent was added dropwise a solution containing 11.5 g (0.043 mol) of 1-(2-methyl-4-methoxyphenyl)-2-(4-methoxyphenyl)ethanone in 125 mL of dry $CHCl_3$. The resulting suspension was stirred for 3 h at room temperature. A mixture of 115 mL of concentrated HCl and 150 mL of H_2O was then carefully added to the reaction mixture. The ether layer was separated and the aqueous layer was washed with ether. The combined ether layers were washed three times with H_2O, dried over anhydrous magnesium sulfate, and filtered and the solvent was removed on a rotary evaporator. The resulting yellow oil crystallizes on standing. The crude product was recrystallized from 200 mL of 95% ethanol to give 6.5 g (59.6%) of white crystals, mp 52–54 °C. Subsequent concentrations of the filtrate and crystallization yielded 3.2 g more product for a total yield of 9.7 g (89.4%). ^{1}H NMR ($CDCl_3$, TMS, δ, ppm) 2.26 (3 protons, CH_3, s), 2.78 (4 protons, CH_2CH_2, s), 3.78 (3 protons, OCH_3 of the unsubstituted phenyl ring, s), 3.79 (3 protons, OCH_3 of the substituted phenyl ring, s), 6.71 (2 protons, ortho to methoxy of the substituted phenyl ring, s and d), 6.83 (2 protons, ortho to methoxy of the unsubstituted phenyl ring, d), 7.03 (1 proton, meta to methoxy of the substituted phenyl ring, d), 7.10 (2 protons, meta to methoxy of the unsubstituted phenyl ring, d). The ^{1}H NMR spectrum shows the product to be 100% pure and free of unreduced ketone.

Synthesis of 1-(4-Hydroxyphenyl)-2-(2-methyl-4-hydroxyphenyl)ethane. This compound was prepared by the demethylation of 1-(4-methoxyphenyl)-2-(2-methyl-4-methoxyphenyl)ethane with BBr_3.[8] A solution of 1-(4-methoxyphenyl)-2-(2-methyl-4-methoxyphenyl)ethane (9.7 g, 0.038 mol) in 150 mL of dry methylene chloride was added dropwise under dry nitrogen atmosphere to 90 mL (0.09 mol) of 1.0 M BBr_3 in methylene chloride cooled in a dry ice–acetone bath. After the mixture was stirred at room temperature for 19 h, enough H_2O was added to hydrolyze the excess BBr_3. During this time a white solid precipitated out of solution. Diethyl ether was added to dissolve this solid, the organic layer was separated, and the aqueous layer was extracted with diethyl ether. The combined organic layers were washed three times with H_2O and dried over anhydrous $MgSO_4$. Evaporation of the solvent in a rotary evaporator yielded 8.0 g (92.6%) white powdery product. The crude product was recrystallized from a 3/2 (v/v) mixture of water/ethanol: purity (HPLC) 99.9%; mp (DSC, 20 °C/min) 148 °C; ^{1}H NMR (acetone-d_6, TMS, δ, ppm) 2.20 (3 protons, CH_3, s), 2.72 (4 protons, CH_2CH_2, s), 6.63 (2 protons, ortho to methoxy of the substituted phenyl ring, s and d), 6.75 (2 protons, ortho to methoxy of the unsubstituted phenyl ring, d), 6.94 (1 proton, meta to methoxy of the substituted phenyl ring, d), 7.02 (2 protons, meta to methoxy of the unsubstituted phenyl ring, d).

Scheme III
Synthesis of Polyethers and Copolyethers Based on 1-(4-Hydroxyphenyl)-2-(2-methyl-4-hydroxyphenyl)ethane and α,ω-Dibromoalkanes

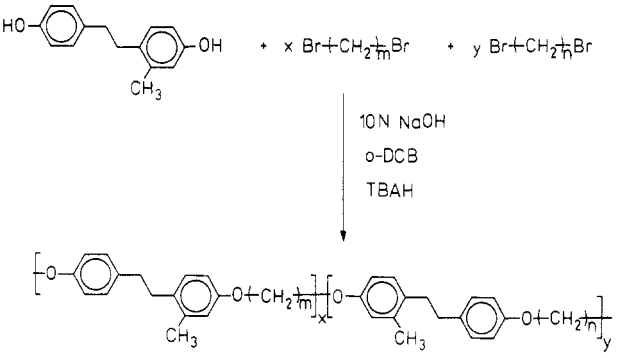

Synthesis of Polyethers and Copolyethers. Synthesis of polyethers and copolyethers based on 1-(4-hydroxyphenyl)-2-(2-methyl-4-hydroxyphenyl)ethane and α,ω-dibromoalkanes is outlined in Scheme III. Conventional liquid–liquid two-phase (organic solvent-aqueous NaOH solution) phase transfer catalyzed polyetherification conditions[9,10] were used for the preparation of the polyethers and copolyethers. The polyetherifications were carried out under nitrogen atmosphere at 80 °C in an *o*-dichlorobenzene–10 N NaOH water solution (10 times molar excess of NaOH versus phenol groups) in the presence of TBAH (10 mol % of phenol groups) as phase transfer catalyst. The ratio of nucleophilic to electrophilic monomers was in every case 1.0/1.0.

An example of copolyetherification is as follows. To a 25-mL single-neck flask equipped with condenser and nitrogen inlet–outlet were successively added 0.2500 g (1.0951 mmol) of 1-(4-hydroxyphenyl)-2-(2-methyl-4-hydroxyphenyl)ethane, 2.2 mL of 10 N NaOH, 0.1413 g (0.5475 mmol) of 1,7-dibromoheptane, 0.1720 g (0.5475 mmol) of 1,11-dibromoundecane, 2 mL of *o*-dichlorobenzene, and 0.0747 g (0.2190 mmol) of TBAH. The reaction mixture was stirred at 1100 rpm with a magnetic stirrer at 80 °C under nitrogen. After 6 h of reaction, the organic and aqueous layers were diluted with chloroform and water, respectively, and the aqueous layer was removed. The organic layer was washed several times with water, followed by dilute hydrochloric acid, and finally with water again. The polymer was separated by precipitation of the polymer solution into methanol to obtain 0.3680 g (93.0%) of white fibrous precipitate. The polymer was further purified by two successive precipitations from chloroform solutions; first into acetone and then into methanol.

In this entire paper the polyethers will be designated MBPE-X where X is the number of methylene units in the spacer. Similarly, copolyethers will be designated MBPE-$X/Y(A/B)$ where X is the number of methylene units in one of the spacers, Y is the number of methylene units in the other, and A/B refers to the molar ratio of the two spacers. Therefore, for example, MBPE-$X/Y(100/0)$ represents MBPE-X.

Techniques. ^{1}H NMR (200-MHz) spectra were recorded on a Varian XL-200 spectrometer.

Molecular weights were determined by gel permeation chromatography (GPC). High-pressure liquid chromatography (HPLC) and GPC analysis were carried out with a Perkin-Elmer Series 10LC equipped with a LC-100 column oven, LC 600 autosampler, and a Sigma 15 data station. The measurements were made by using the UV detector, tetrahydrofuran as solvent (1 mL/min, 40 °C), a set of PL gel columns of 10^2, 5×10^2, 10^3, 10^4, and 10^5 Å, and a calibration plot constructed with polystyrene standards.

A Perkin-Elmer DSC-4 differential scanning calorimeter equipped with a TADS data station Model 3600 was used to determine the thermal transitions. Heating and cooling rates were 20 °C/min in all cases unless stated. First-order transitions

(crystalline–crystalline, crystalline–liquid crystalline, liquid crystalline–isotropic, etc.) were read at the maximum of the endothermic or exothermic peaks. Glass transition temperatures (T_g) were read at the middle of the change in the heat capacity. All heating and cooling scans after the first heating scan produced perfectly reproducible data. The transitions reported were taken from the second or third heating or cooling scans. As discussed in detail in the results and discussion section, different thermal histories are strongly influencing the thermal behavior of these polymers.

A Carl Zeiss optical polarizing microscope (magnification 100×) equipped with a Mettler FP 82 hot stage and a Mettler 800 central processor was used to observe the thermal transitions and to analyze the textures.[11]

Results and Discussion

The polyethers and copolyethers described in this paper are soluble in conventional solvents such as chloroform, tetrahydrofuran, etc. Their molecular weights were determined by GPC using polystyrene as calibration standards and therefore have only a relative meaning. Nevertheless, they are useful in deciding whether phase transitions of different polymers can be compared. Previously, we have shown that for polyethers with number-average molecular weights below 12 000, liquid crystalline transitions are strongly influenced by the nature of the polymer chain ends.[10,12] For polymers with higher molecular weights, liquid crystalline transitions are kinetically controlled.[13] Therefore, in contrast to what most of the researchers in this field have assumed, equilibrium values require a more careful consideration of all these parameters.[13]

Since the polymer systems discussed here should exhibit a dynamic behavior due to the nature of their mesogenic units, in this first manuscript we will discuss mostly data taken from DSC heating and cooling scans recorded at 20 °C/min. The influence of sample thermal history on phase behavior will only be briefly mentioned since it will represent the subject of future publications. Therefore, for the accuracy of this discussion we are mostly concerned with having polymers of number-average molecular weights between 20 000 and 30 000 and of accurate composition. Since in all cases the yields were as high as 90% or higher, we can assume that conversions were close to 100% and consequently it is quite correct to consider that each copolymer composition is identical with that of the monomer feed composition. An additional point of concern refers to the copolymer sequence distribution. The reactivities of the two phenolate groups in MBPE should not be very different. At the same time we assume that the reactivities of the leaving groups in the α,ω-dibromoalkanes should not be dependent on the number of methylene units. Therefore, for the purpose of this discussion, we can safely assume that we are dealing with statistical copolymers.

In the first part of the discussion that follows, we will present the phase behavior of the homopolymers as can be determined from their own DSC thermograms. In the second part, we will discuss the phase behavior of their corresponding copolymers. The conclusions resulting from the second part will allow not only phase diagrams to be determined for the copolymers but also the determination of virtual phase transitions to be made for the homopolymers. As we have previously stated, most of the results refer to perfectly reproducible heating and cooling DSC thermograms (20 °C/min) which are recorded from second or subsequent scans.

The second heating scan for MBPE-5 is presented on the top of Figure 1a while the corresponding cooling scan is on the top of Figure 1b. Liquid crystalline transitions are much less kinetically controlled than the crystalline

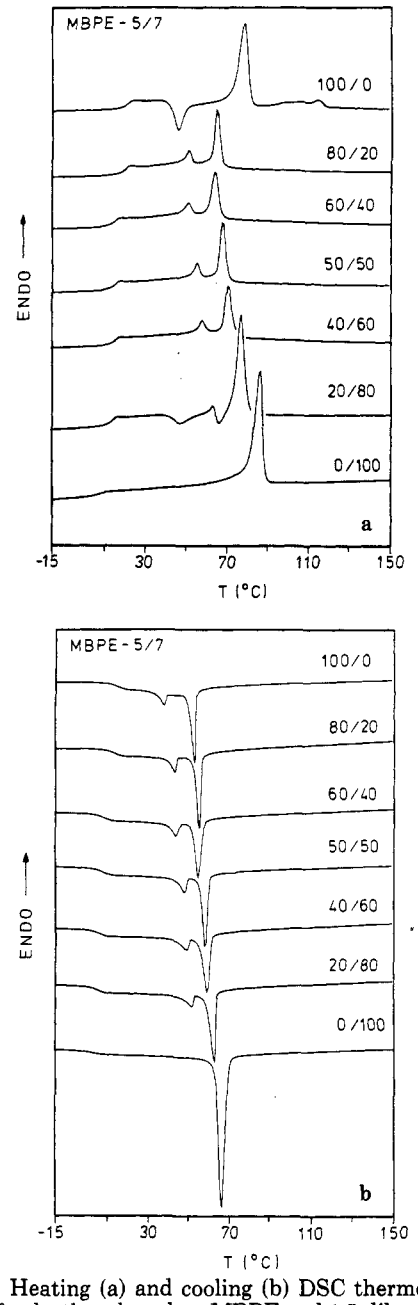

Figure 1. Heating (a) and cooling (b) DSC thermograms (20 °C/min) of polyethers based on MBPE and 1,5-dibromopentane (MBPE-5), MBPE and 1,7-dibromoheptane (MBPE-7), and corresponding copolyethers [MBPE-5/7(A/B)].

transitions. Therefore, liquid crystalline transitions observed on the cooling scan are only slightly supercooled versus the corresponding transitions on the heating scan and their enthalpic changes are always slightly lower when determined from the cooling thermograms.[9] For the sake of simplicity, it is easier to discuss first the cooling scan (Figure 1b). This polymer undergoes an isotropic–nematic transition at 51 °C and a nematic-smectic transition at 37 °C. The nematic mesophase can be easily identified through the value of its corresponding enthalpy change (Table I) and the typical nematic threaded texture observed by optical polarized microscopy. However, a typical smectic texture cannot be obtained because the polymer crystallizes during the annealing time on the hot stage of the optical microscope. The same comment is valid for the optical characterization of the nematic–smectic transition in the other homopolymers. As will be discussed later, at the nematic–smectic transition there is a change in the mesophase which can be observed in most of the

Table I
Characterization of Polyethers Based on MBPE and 1,5-Dibromopentane (MBPE-5), MBPE, and 1,7-Dibromoheptane (MBPE-7) and of Corresponding Copolyethers [MBPE-5/7(*A*/*B*)]

copolymer MBPE-5/7(*A*/*B*) 5/7 mol ratio	$\bar{M}_n$	$\bar{M}_w/\bar{M}_n$	thermal transitions, °C, and corresponding enthalpy changes (kcal/mru) in parentheses: heating	cooling
100/0	19000	1.90	g 20 k 79 (1.44) k 115 (0.33) i	i 51 (0.57) n 37 (0.10) s 13 g
80/20	21700	1.77	g 19 s 51 (0.15) n 65 (0.58) i	i 55 (0.61) n 43 (0.16) s 12 g
60/40	22500	1.73	g 14 s 51 (0.15) n 64 (0.57) i	i 54 (0.60) n 43 (0.16) s 7 g
50/50	20700	1.85	g 14 s 55 (0.16) n 68 (0.62) i	i 58 (0.65) n 48 (0.17) s 7 g
40/60	25300	1.73	g 14 s 58 (0.13) n 70 (0.62) i	i 59 (0.64) n 48 (0.17) s 6 g
20/80	24800	1.96	g 13 k 63 (0.11) k 77 (1.55) i	i 62 (0.71) n 51 (0.15) s 5 g
0/100	22100	1.76	g 7 k 85 (2.18) i	i 66 (2.01) k 0 g

Table II
Characterization of Virtual Liquid Crystalline Transitions and Thermodynamic Parameters [ ] for Homopolymers (MBPE-X) and Copolyethers [MBPE-*X*/*Y*(*A*/*B*)]

copolymer MBPE-*X*/*Y*	*X*/*Y* mol ratio	thermal transitions, °C, and the corresponding enthalpy changes (kcal/mru) in parentheses: heating	cooling
MBPE-5/7	100/0	g 20 s [46 (0.16)] n [61 (0.55)] k 79 (1.44) k 115 (0.33) i	i 51 (0.57) n 37 (0.10) s 13 g
	20/80	g 13 s [60 (0.14)] k 63 (0.11) n [72 (0.64)] k 77 i	i 62 (0.71) n 51 (0.15) s 5 g
	0/100	g 7 s [64 (0.13)] n [75 (0.66)] k 85 (2.18) i	i 66 (2.01) k [64 (0.72)] n [55 (0.17)] s 0 g
MBPE-5/9	100/0	g 20 s [44 (0.14)] n [56 (0.45)] k 79 (1.44) k 115 (0.33) i	i 51 (0.57) n 37 (0.10) s 13 g
	20/80	g 6 k 62 s [66 (0.14)] k 74 n 80 (1.17[a]) i	i 64 (0.81) n 54 (0.11) s 1 g
	0/100	g 6 s [71 (0.14)] k 75 k 80 n [85 (0.88)] k 91 (4.02) i	i 64 (1.05) n 58 (0.06) s 48 (2.13) k 0 g
MBPE-5/11	100/0	g 20 s [48 (0.13)] n [63 (0.31)] k 79 (1.44) k 115 (0.33) i	i 51 (0.57) n 37 (0.10) s 13 g
	20/80	g 13 k 57 (0.41) s [71 (0.07)] n [80 (1.14)] k 89 (3.07) i	i 69 (1.09) n 62 (0.06) s 32 (0.42) k 4 g
	0/100	g 5 s [76 (0.05)] n [85 (1.35)] k 101 (5.21) i	i 72 (1.09) n [69 (0.08)] s 64 (2.66) k
MBPE-7/9	100/0	g 7 s [60 (0.14)] n [73 (0.64)] k 85 (2.18) i	i 66 (2.01) k [66 (0.77)] n [58 (0.19)] s 0 g
	80/20	g 11 s [62 (0.14)] k 64 (0.21) n [74 (0.73)] k 79 (1.91) i	i 67 (0.85) n 58 (0.14) s 38 (0.09) k 3 g
	20/80	g 9 k 50 (0.23) k 67 (0.06) s [67 (0.14)] n [79 (1.00)] k 82 (1.91) i	i 70 (0.98) n 60 (0.14) s 2 g
	0/100	g 6 s [70 (0.14)] k 75 k 80 n [81 (1.09)] k 91 (4.02) i	i 69 (1.05) n 58 (0.06) s 48 (2.13) k 0 g
MBPE-7/11	100/0	g 7 s [68 (0.19)] n [80 (0.47)] k 85 (2.18) i	i 66 (2.01) k [66 (0.78)] n [58 (0.11)] s 0 g
	80/20	g 10 k 62 (0.13) s [68 (0.16)] n [79 (0.66)] k 79 (1.72) i	i 68 (0.87) n 60 (0.15) s 5 g
	20/80	g 13 k 49 (0.14) s [69 (0.07)] n [79 (1.23)] k 91 (3.30) i	i 72 (1.16) n 64 (0.15) s 34 (0.37) k 6 g
	0/100	g 5 s [69 (0.04)] n [79 (1.42)] k 101 (5.21) i	i 72 (1.09) n 64 (2.66) k [64 (0.14)] s
MBPE-9/11	100/0	g 6 n [73] k 75 k 80 k 91 (4.02) i	i 69 (1.05) n 58 (0.06) s 48 (2.13) k 0 g
	80/20	g 10 k 47 (0.30) n [76] k 77 k 86 (2.80[a]) i	i 72 (1.12) n 63 (0.15) s 19 (0.12) k 3 g
	20/80	g 11 k 52 (0.16) k 72 k 81 n [86] k 89 (3.19[a]) i	i 71 (1.25) n 63 (0.10) s 41 (1.11) k 5 g
	0/100	g 5 n [89] k 101 (5.21) i	i 72 (1.09) n [66 (0.11)] s 64 (2.66) k

[a] Overlapping transitions.

Table III
Characterization of Polyethers Based on MBPE and 1,5-Dibromopentane (MBPE-5) and 1,9-Dibromononane (MBPE-9) and of Corresponding Copolyethers [MBPE-5/9(*A*/*B*)]

copolymer MBPE-5/9(*A*/*B*) 5/9 mol ratio	$\bar{M}_n$	$\bar{M}_w/\bar{M}_n$	thermal transitions, °C, and corresponding enthalpy changes (kcal/mru) in parentheses: heating	cooling
100/0	19000	1.90	g 20 k 79 (1.44) k 115 (0.33) i	i 51 (0.57) n 37 (0.10) s 13 g
80/20	24300	1.80	g 15 s 51 (0.13) n 64 (0.54) i	i 53 (0.58) n 42 (0.15) s 7 g
60/40	20100	1.63	g 11 s 54 (0.15) n 66 (0.62) i	i 57 (0.65) n 47 (0.17) s 4 g
50/50	18100	1.66	g 9 s 56 (0.14) n 68 (0.67) i	i 60 (0.72) n 49 (0.17) s 2 g
40/60	30200	1.76	g 11 s 62 (0.13) n 74 (0.71) i	i 62 (0.69) n 53 (0.10) s 2 g
20/80	26700	2.01	g 9 k 62 k 74 n 80 (1.17[a]) i	i 64 (0.81) n 54 (0.11) s 1 g
0/100	20600	1.38	g 6 k 75 k 80 k 91 (4.02) i	i 64 (1.05) n 58 (0.06) s 48 (2.13) k 0 g

[a] Overlapping transitions.

copolymers. Although additional evidence for this "smectic" mesophase is going to be collected over the entire paper, direct evidence for this mesophase requires X-ray scattering experiments. On the DSC heating scan of MBPE-5 (Figure 1a), we observe a crystallization exotherm immediately after T_g, followed by melting endotherms at 79 and 115 °C. No liquid crystalline transition could be observed on the heating scan by optical polarized microscopy. Therefore, MBPE-5 exhibits two monotropic mesophases. The ratio between the enthalpy changes associated with these two melting endotherms is strongly dependent on the thermal history of the sample. As obtained after precipitation from solution or after annealing at room temperature (25 °C) for 4 weeks, the DSC thermogram of MBPE-5 no longer exhibits a glass transition or a melting endotherm at 79 °C. At the same time, the melting endotherm at 115 °C is accompanied by a much larger enthalpy change.

On the heating scan, MBPE-7 presents a glass transition at 7 °C and a single melting endotherm at 85 °C (Figure 1a). A single crystallization exotherm at 66 °C followed by a T_g at 0 °C is observed on the cooling scan of the same sample (Figure 1b) (Table I). Upon annealing at room temperature, the melting enthalpy increases and the peak gets split into several endotherms which could not be separated into individual peaks and therefore were not analyzed independently. Consequently, MBPE-7 is a crystalline polymer.

Heating (Figure 2a) and cooling (Figure 2b) DSC thermograms of MBPE-9 were analyzed in the same way

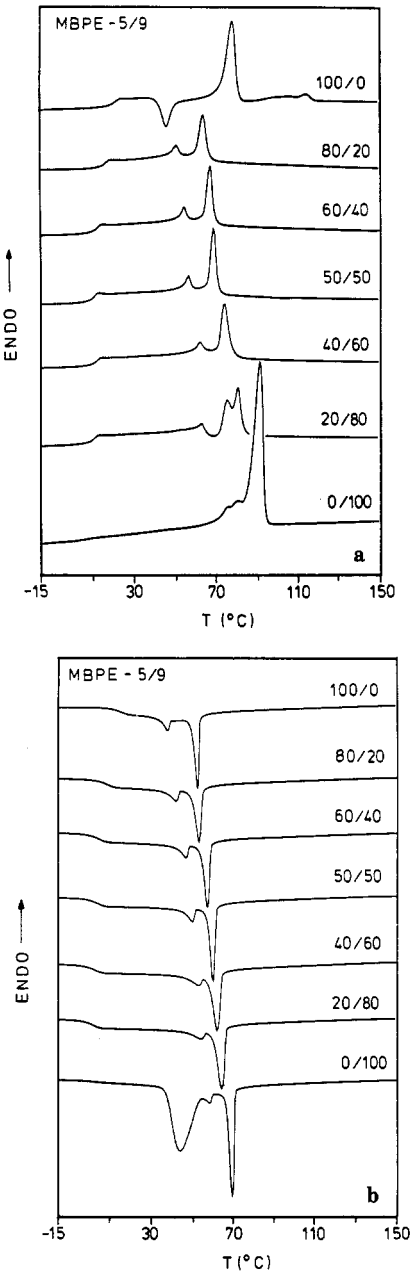

Figure 2. Heating (a) and cooling (b) DSC thermograms (20 °C/min) of polyethers based on MBPE and 1,5-dibromopentane (MBPE-5), MBPE and 1,9-dibromononane (MBPE-9), and corresponding copolyethers [MBPE-5/9(A/B)].

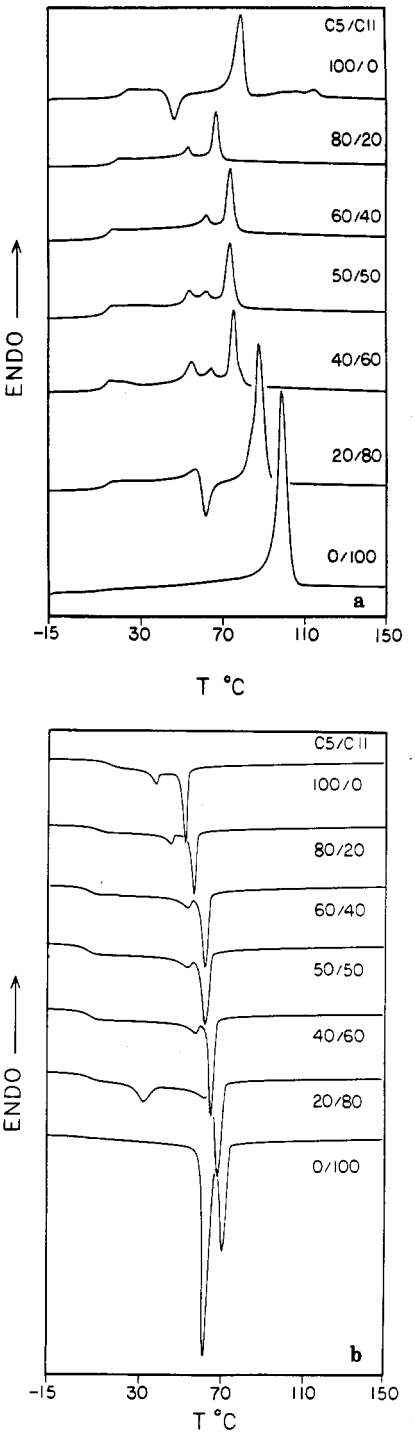

Figure 3. Heatigng (a) and cooling (b) DSC thermograms (20 °C/min) of polyethers based on MBPE and 1,5-dibromopentane (MBPE-5), MBPE and 1,11-dibromoundecane (MBPE-11), and corresponding copolyethers [MBPE-5/11(A/B)].

(Tables II and III). They led to the conclusion that this polymer exhibits on heating three crystalline meltings at 75, 80, and 91 °C and on cooling an isotropic-nematic transition at 69 °C, a nematic-smectic transition at 58 °C, and a crystallization exotherm at 48 °C. The nematic mesophase exhibits a typical threaded texture while the smectic mesophase is metastable and undergoes crystallization due its close proximity to the crystallization exotherm (Figure 2b). The heating DSC thermogram of MBPE-9 as precipitated from solution or upon annealing at room temperature for 4 weeks exhibits additional melting endotherms which will not be discussed in this paper.

Finally, MBPE-11 displays a melting endotherm at 101 °C on the heating DSC scan (Figure 3a) and an isotropic-nematic transition at 72 °C followed by crystallization at 64 °C on the cooling DSC scan (Figure 3b) (Tables II and IV). As annealed at room temperature for about 4 weeks or as precipitated from solution, MBPE-11 presents on its DSC thermogram additional melting endotherms which will be described in another publication.

In conclusion, according to DSC and thermal optical polarized microscopy measurements, both MBPE-5 and MBPE-9 display nematic and smectic monotropic mesophases, MBPE-11 exhibits a nematic monotropic mesophase, and MBPE-7 is only crystalline.

In order to understand the relationship between the composition of copolymers obtained from a single mesogenic unit and two different spacers and their phase behavior, we have synthesized MBPE-X/Y copolymers from each pair of odd-numbered spacers, i.e., X = 5, 7, 9, 11 and Y = 5, 7, 9, 11. Recent work on the same subject performed in different laboratories leads to the conclusion that

Table IV
Characterization of Polyethers Based on MBPE and 1,5-Dibromopentane (MBPE-5) and 1,11-Dibromoundecane (MBPE-11) and of Corresponding Copolyethers [MBPE-5/11(A/B)]

copolymer MBPE-5/11(A/B) 5/11 mol ratio	$\bar{M}_n$	$\bar{M}_w/\bar{M}_n$	thermal transitions, °C, and the corresponding enthalpy changes (kcal/mru) in parentheses: heating	cooling
100/0	19000	1.90	g 20 k 79 (1.44) k 115 (0.33) i	i 51 (0.57) n 37 (0.10) s 13 g
80/20	22600	1.89	g 16 s 53 (0.10) n 66 (0.50) i	i 56 (0.53) n 45 (0.12) s 9 g
60/40	25400	1.83	g 12 s 61 (0.13) n 73 (0.75) i	i 62 (0.75) n 53 (0.11) s 5 g
50/50	27370	1.87	g 12 k 54 s 62 (0.07) 73 (0.86) i	i 62 (0.88) n 53 (0.09) s 4 g
40/60	27600	1.81	g 12 k 55 (0.25) s 64 (0.08) n 75 (0.90) i	i 66 (0.92) n 57 (0.12) s 5 g
20/80	25000	2.11	g 13 k 57 (0.41) k 89 (3.07) i	i 69 (1.09) n 62 (0.06) s 32 (0.42) k 4 g
0/100	28500	2.02	g 5 k 101 (5.21) i	i 72 (1.09) n 64 (2.66) k

copolymerization depresses crystallization transition temperatures as well as their enthalpy changes determined in a dynamic way. At the same time, liquid crystalline transitions and their enthalpy changes are weight-averaged over those of the parent homopolymers.[9,14-18]

This conclusion can be used as an important experimental tool to obtain further information about the phase behavior of both homopolymers and copolymers. First, by weight-averaging liquid crystalline transitions of copolymers and their enthalpy changes, we can obtain information about eventual virtual transitions and enthalpies of their parent homopolymers which displayed only crystalline transitions.[17]

Since three out of our four homopolymers exhibit monotropic phase transitions, we believe that copolymerization experiments might first elucidate if MBPE-7 is only crystalline or whether it exhibits virtual monotropic liquid crystalline transitions. Alternatively, as it has been already demonstrated,[9] copolymerization depresses crystalline transitions and transforms monotropic mesophases into enantiotropic mesophases. Subsequently, if this will be the case, by copolymerization we might be able to obtain information about possible enantiotropic virtual mesophases exhibited by all four homopolymers.

Figure 1a presents the heating scans and Figure 1b the cooling scans of the DSC thermograms of the copolymers series MBPE-5/7. The thermal transitions and their corresponding enthalpy changes are collected in Table I. A single comment must be made at this point. In general, the enthalpy changes calculated from the cooling scans are slightly lower than those of the heating scans.[9] However, all the data calculated from the polymers presented in this paper present an inverse trend. That is the enthalpy changes from the heating scans are lower than from the cooling scans. This is due to the better separation of the corresponding peaks on the cooling scans. When plotted as a function of copolymer composition, a single line passes through heating and cooling enthalpies. When calculated, there are lines corresponding to each set of data. On the scale of our figures, these two lines will always overlap and are shown as a single line. However, when tabulated, two sets of extrapolated data appear.

Thermal transitions are plotted as a function of copolymer composition in Figure 4b while their corresponding enthalpy changes are plotted in Figure 4b. A close inspection of the data collected from the cooling scans in Figure 1b and plotted in Figures 4a and 4b leads to an expected conclusion. The isotropic–nematic and nematic–smectic transitions obtained from the cooling scans (Figure 4a) and their corresponding enthalpy changes (Figure 4b) are a linear function of composition, therefore representing the weighted average of the corresponding quantities of the homopolymers. The extrapolation of both thermal transitions and of the corresponding enthalpies

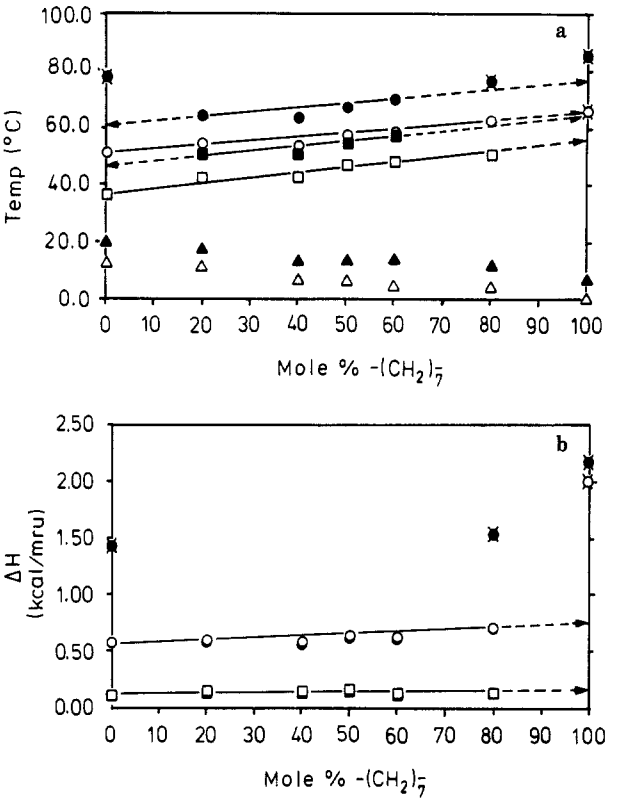

Figure 4. (a) Thermal transitions for homopolymers (MBPE-5 and MBPE-7) and copolymers [MBPE-5/7(A/B)]: (●) T_{ni}; (○) T_{in}; (✖) T_{ki}; (○) T_{ik}; (■) T_{sn}; (□) T_{ns}; (▲) T_g(heating); (△) T_g(cooling). Arrows point to virtual transitions for the homopolymers. (b) Enthalpy changes for homopolymers (MBPE-5 and MBPE-7) and copolymers [MBPE-5/7(A/B)]: (●) ΔH_{ni}; (○) ΔH_{in}; (✖) ΔH_{ki}; (⊠) ΔH_{ik}; (■) ΔH_{sn}; (□) ΔH_{ns}. Arrows point to enthalpies of virtual transitions for the homopolymers.

for the homopolymer MBPE-7 shows that this homopolymer has a virtual isotropic–nematic transition at 64 °C with a corresponding enthalpy of 0.72 kcal/mru and a virtual nematic-smectic transition at 55 °C with a corresponding enthalpy of 0.17 kcal/mru (Figure 4 and Table II). We can see from Figure 4b that as expected, enthalpy changes associated with liquid crystalline transitions determined from the heating and cooling scans are identical. Those enthalpies which do not form a linear relation versus composition are represented by crossed markers. Although their corresponding thermal transitions are almost weight averaged, the disagreement between these two linear relationships assumes that the crossed transition markers do not belong to liquid crystalline transitions and therefore should be considered to represent crystalline transitions. This conclusion is supported by the observation of these copolymers on the hot plate of the optical polarized microscope. Consequently, as suspected, copolymerization depresses crystalline transition temperatures and trans-

forms monotropic mesophases into enantiotropic mesophases. The extrapolation of the linear dependence of these monotropic liquid crystalline transitions (Figures 1a and 4) and enthalpy changes to the corresponding homopolymers gives the following results. MBPE-5 displays on the heating scan a virtual smectic–nematic transition at 46 °C (ΔH_{sn} = 0.16 kcal/mru) and a virtual nematic–isotropic transition at 61 °C (ΔH_{ni} = 0.55 kcal/mru). MBPE-7 exhibits a virtual smectic–nematic transition at 64 °C (ΔH_{sn} = 0.13 kcal/mru) and a virtual nematic–isotropic transition at 75 °C (ΔH_{ni} = 0.66 kcal/mru). This analysis allows the determination of the virtual transitions also for the crystalline copolymers as for example for MBPE-5/7(20/80) (Table II).

The DSC scans of the MBPE-5/9 copolymer series are presented in Figure 2a (heating scans) and Figure 2b (cooling scans). The quantitative data for this set of copolymers are summarized in Table III. The DSC traces for the cooling scans represent an ideal example of the linear dependence of phase transitions and their corresponding thermodynamic parameters versus copolymer composition (Figure 2b). This is because both MBPE-5 and MBPE-9 present nematic and smectic monotropic mesophases. The thermal transition temperatures corresponding to isotropic–nematic and nematic–smectic are situated on perfect straight lines which definitively demonstrate that liquid crystalline transitions of copolymers are weight-averaged values of the corresponding transitions of the parent homopolymers. The same is true for the enthalpy changes associated with these transitions (Figure 5b). An important remark is that insertion of as little as 20% of the short spacer within the structure of MBPE-5/9 copolymers suppresses completely copolymer crystallization (Figure 2b). Analysis of the phase transitions collected from the heating scans (Figure 2a) was done by comparing the correspondence between the linearity of the phase transition temperatures (Figure 5a) and that of their enthalpy changes (Figure 5b). These plots led to the conclusion that the crossed data markers from both parts a and b of Figure 5 are due to crystalline transitions. However, the extrapolation of T_{sn} and T_{ni} from the heating scans led to the determination of the smectic–nematic and nematic–isotropic virtual transitions for both MBPE-5 and MBPE-9. The extrapolation of the corresponding enthalpy changes associated with T_{sn} and T_{ni} from the heating scans was done as for the previously analyzed MBPE-5/7 copolymers and leads to similar values of the enthalpy changes regardless of whether the data were obtained from heating or cooling scans. As we can observe from the results summarized in Table II, the virtual transition temperatures determined for MBPE-5 from the MBPE-5/7 copolymers and MBPE-5/9 copolymers agree very well. However, a more detailed discussion on the virtual phase transitions determined from different sets of experiments will be made at the end of this paper.

The copolymer system MBPE-5/11 represents a situation which is intermediary between the behavior of copolymers MBPE-5/7 and MBPE-5/9. That is, while both MBPE-5 and MBPE-9 exhibit nematic and smectic monotropic mesophases, MBPE-7 is only crystalline. At the same time, MBPE-11 displays only a nematic monotropic mesophase. Heating and cooling DSC thermograms for the MBPE-5/11 copolymer system are presented in Figure 3. The quantitative data corresponding to the thermal transitions collected from these DSC thermograms are reported in Table IV. Again the DSC traces recorded on cooling can be interpreted in a straightforward manner. The nematic–crystalline transition of MBPE-11 is dramatically depressed in MBPE-5/11(20/80) and disappears in copolymers containing larger amounts of the shorter spacer. The isotopic–nematic transition is plotted in Figure 6a and demonstrates a linear relationship between the temperature of this transition and the copolymer composition. The same conclusion is valid for the enthalpy changes associated with the isotropic–nematic transitions (Figure 6b). The nematic–smectic transitions give also a straight line which by extrapolation to MBPE-11 gives a virtual nematic–smectic temperature transition of 69 °C with an enthalpy change of 0.08 kcal/mru (Table II). On the heating scan, for the copolymers with compositions from MBPE-5/11(80/20) to MBPE-5/11(40/60), both the monotropic smectic–nematic and nematic–isotropic transitions become enantiotropic (Figures 3a and 6). The extrapolation of the linear dependence between phase transition temperatures and their enthalpies versus composition led to the determination of the virtual smectic–nematic transition for MBPE-11 and of the virtual nematic–isotropic transition for both MBPE-5 and MBPE-11. These transitions as well as their corresponding enthalpy changes are reported in Table II.

The copolymer system MBPE-7/9 resembles the situation of the copolymer system MBPE-5/7. However, in this case the homopolymer containing the short spacer (MBPE-7) is crystalline while the homopolymer containing the long spacer (MBPE-9) exhibits two monotropic mesophases (nematic and smectic) and a crystallization transition on cooling. The DSC traces of the heating and

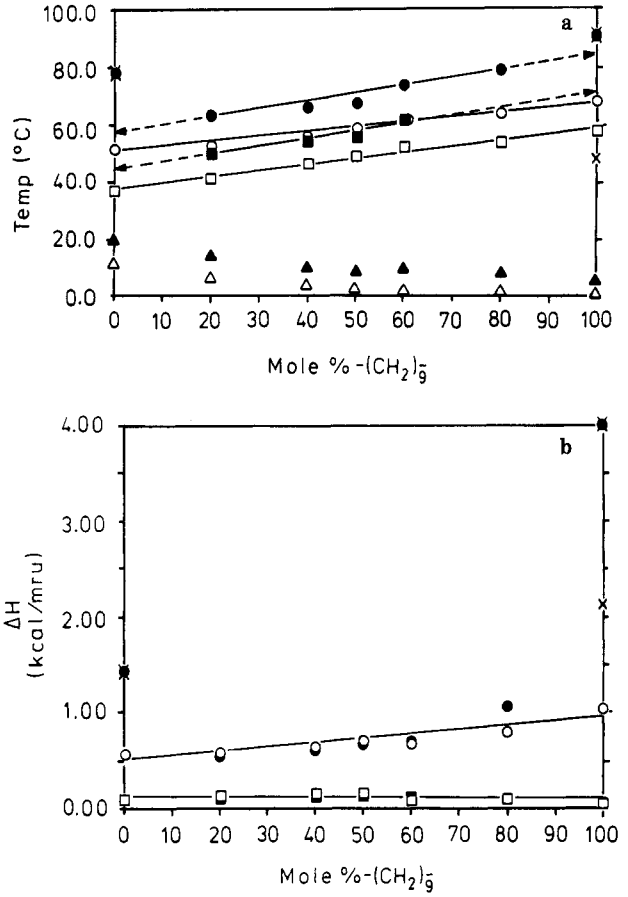

Figure 5. (a) Thermal transitions for homopolymers (MBPE-5 and MBPE-9) and copolymers [MBPE-5/9(A/B)]: (●) T_{ni}; (○) T_{in}; (▣) T_{ki}; (■) T_{sn}; (□) T_{ns}; (×) T_{sk}; (▲) T_g(heating); (△) T_g(cooling). Arrows point to virtual transitions for the homopolymers. (b) Enthalpy changes for homopolymers (MBPE-5 and MBPE-9) and copolymers [MBPE-5/9(A/B)]: (●) ΔH_{ni}; (○) ΔH_{in}; (▣) ΔH_{ki}; (■) ΔH_{sn}; (□) ΔH_{ns}; (×) ΔH_{sk}. Arrows point to enthalpies of virtual transition for the homopolymers.

Table V
Characterization of Polyethers Based on MBPE and 1,7-Dibromoheptane (MBPE-7) and 1,9-Dibromononane (MBPE-9) and of Corresponding Copolyethers [MBPE-7/9(*A*/*B*)]

copolymer MBPE-7/9(*A*/*B*) 7/9 mol ratio	$\bar{M}_n$	$\bar{M}_w/\bar{M}_n$	thermal transitions, °C, and the corresponding enthalpy changes (kcal/mru) in parentheses: heating	cooling
100/0	22100	1.76	g 7 k 85 (2.18) i	i 66 (2.01) k 0 g
80/20	29100	2.04	g 11 k 62 (0.21) k 79 (1.91) i	i 67 (0.85) n 58 (0.14) s 38 (0.09) k 3 g
60/40	26600	1.94	g 8 s 63 (0.14) n 75 (0.80) i	i 67 (0.84) n 57 (0.17) s 3 g
50/50	29100	1.87	g 9 s 66 (0.15) n 78 (0.89) i	i 68 (0.91) n 59 (0.15) s 2 g
40/60	23000	1.64	g 8 s 65 (0.14) n 77 (0.89) i	i 68 (0.91) n 59 (0.16) s 2 g
20/80	27000	1.84	g 9 k 50 (0.23) k 67 (0.06) k 82 (1.91) i	i 70 (0.98) n 60 (0.14) s 2 g
0/100	20600	1.38	g 6 k 75 k 80 k 91 (4.02) i	i 69 (1.05) n 58 (0.06) s 48 (2.13) k 0 g

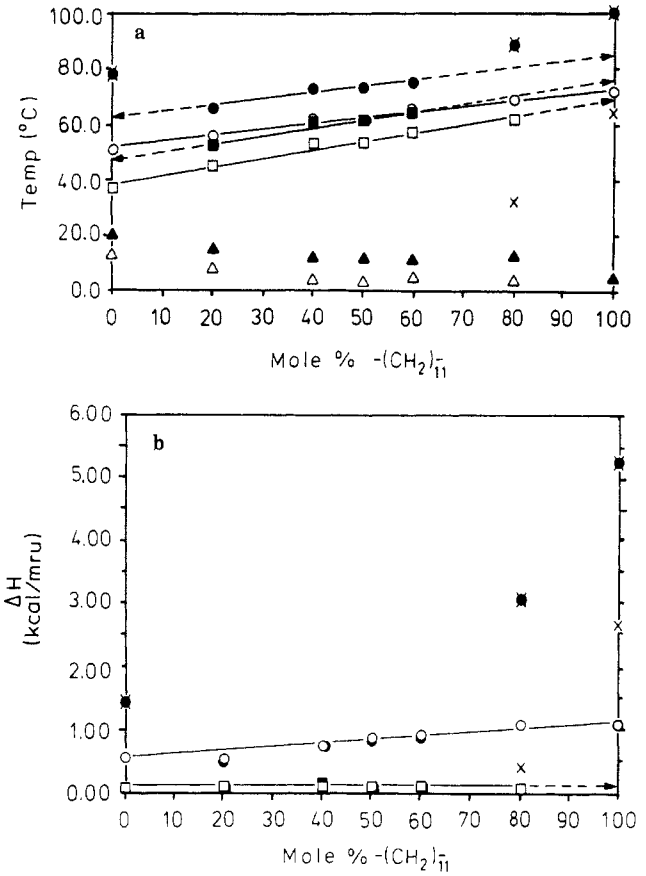

Figure 6. (a) Thermal transitions for homopolymers (MBPE-5 and MBPE-11) and copolymers [MBPE-5/11(*A*/*B*)]: (●) T_{ni}; (○) T_{in}; (◙) T_{ki}; (■) T_{sn}; (□) T_{ns}; (×) T_{sk} or T_{nk}; (▲) T_g(heating); (△) T_g(cooling). Arrows point to virtual transitions for the homopolymers. (b) Enthalpy changes for homopolymers (MBPE-5 and MBPE-11) and copolymers [MBPE-5/11(*A*/*B*)]: (●) ΔH_{ni}; (○) ΔH_{in}; (◙) ΔH_{ki}; (■) ΔH_{sn}; (□) ΔH_{ns}; (×) ΔH_{nk} or ΔH_{sk}. Arrows point to enthalpies of virtual transitions for the homopolymers.

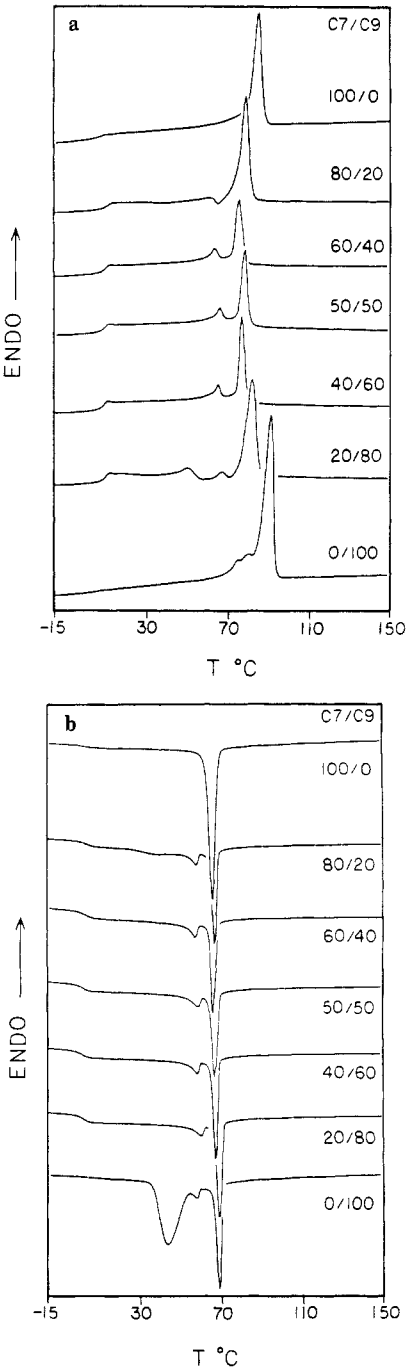

Figure 7. Heating (a) and cooling (b) DSC thermograms (20 °C/min) of polyethers based on MBPE and 1,7-dibromoheptane (MBPE-7), MBPE and 1,9-dibromononane (MBPE-9), and corresponding copolyethers [MBPE-7/9(*A*/*B*)].

cooling scans are presented in Figure 7 and their quantitative data are reported in Table V.

As in all previous examples of copolymers, it is easier to begin by discussing the cooling DSC thermograms. The insertion of as little as 20 mol % short spacer within the MBPE-7/9 copolymer suppresses completely copolymer crystallization. However, 20 mol % of long spacer only depresses [MBPE-7/9(80/20)] copolymer crystallization. All the copolymers with composition from MBPE-7/9-(60/40) to MBPE-7/9(20/80) do not crystallize when the cooling rate is 20 °C/min. The nematic and smectic monotropic liquid crystalline transitions follow a linear dependence on composition and upon extrapolation to MBPE-7 (Figure 8a) lead to the virtual isotropic–nematic and nematic–smectic transitions reported in Table II. The extrapolation of the corresponding enthalpies (Figure 8b) to the virtual enthalpies for MBPE-7 are also reported in Table II. The thermal transitions and corresponding enthalpies collected from the heating scans are plotted in Figure 8. Analysis of these data based on the linearity of

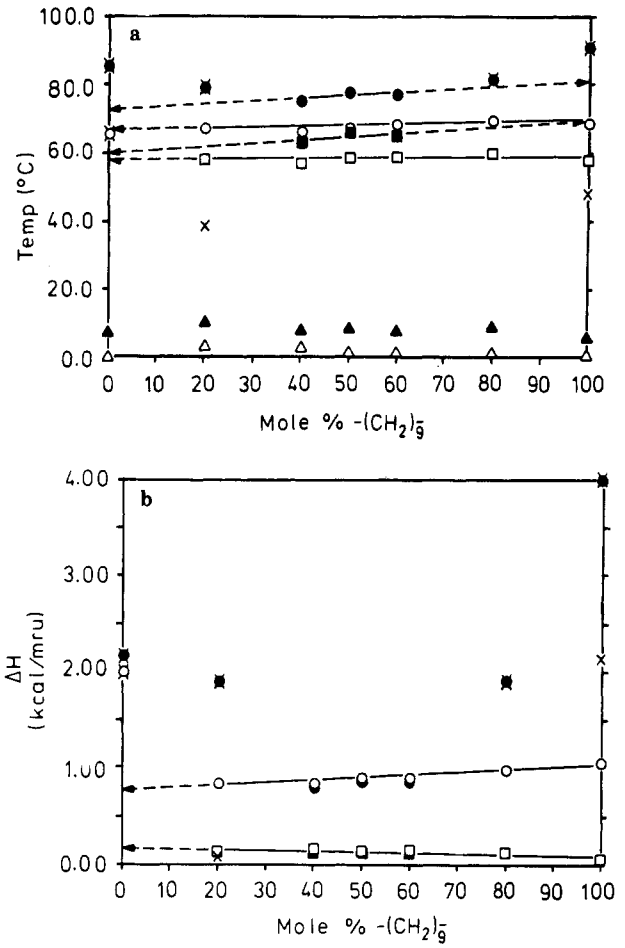

Figure 8. (a) Thermal transitions for homopolymers (MBPE-7 and MBPE-9) and copolymers [MBPE-7/9(A/B)]: (●) T_{ni}; (○) T_{in}; (▣) T_{ki}; (○) T_{ik}; (■) T_{sn}; (□) T_{ns}; (×) T_{sk}; (▲) T_g(heating); (△) T_g(cooling). Arrows point to virtual transitions for the homopolymers. (b) Enthalpy changes for homopolymers (MBPE-7 and MBPE-9) and copolymers [MBPE-7/9(A/B)]: (●) ΔH_{ni}; (○) ΔH_{in}; (▣) ΔH_{ki}; (○) ΔH_{ik}; (■) ΔH_{sn}; (□) ΔH_{ns}; (×) ΔH_{sk}. Arrows point to enthalpies of virtual transitions for the homopolymers.

both enthalpic changes and thermal transition temperatures shows that MBPE-7/9(60/40) to MBPE-7/9(40/60) exhibit enantiotropic nematic mesophases. The smectic mesophase becomes enantiotropic over the range of composition MBPE-7/9(20/80) to MBPE-7/9(80/20) (Figure 8a). The extrapolation of both thermal transitions and their corresponding enthalpy changes led to the virtual smectic–nematic and nematic–isotropic transition temperatures and thermodynamic parameters reported in Table II.

Although the analysis of these copolymer systems tends to become a straightforward experiment, the following two sets of copolymers will still provide completely unique situations in comparison with the previously discussed copolymers.

For example, starting from parent homopolymers which are crystalline (MBPE-7) and monotropic nematic (MBPE-11), respectively, by copolymerization we will demonstrate that both homopolymers exhibit not only virtual nematic but also virtual smectic mesophases. The heating and cooling DSC thermograms for this system are presented in Figure 9 with the quantitative thermal data collected in Table VI. Let us first discuss the DSC thermograms obtained on cooling. Addition of 20 mol % of short spacer in a copolymer depresses the crystallization transition and allows the smectic mesophase to be observed in MBPE-7/11(20/80) (Figure 9b). Insertion of 20 mol % of long spacer suppresses crystallization and allows both

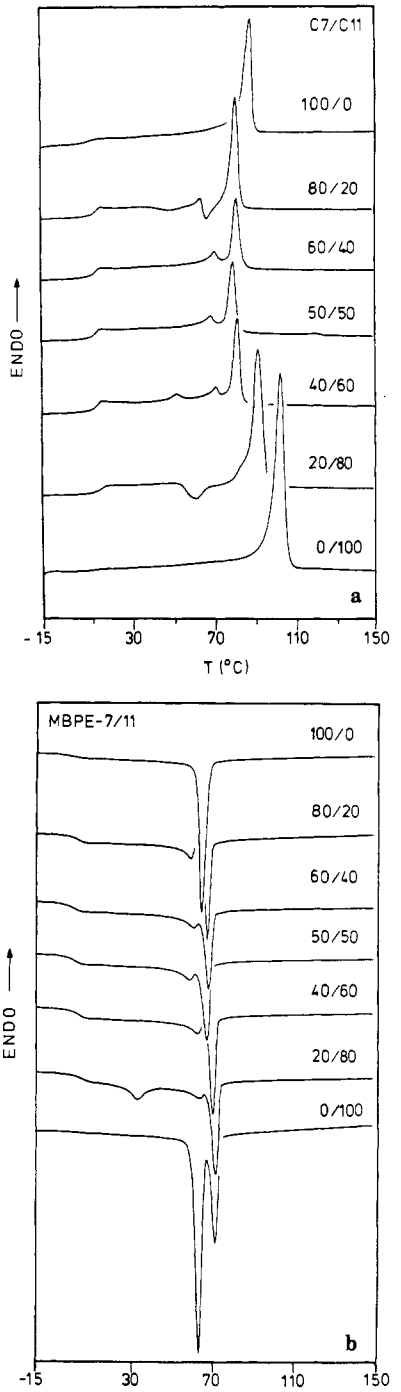

Figure 9. Heating (a) and cooling (b) DSC thermograms (20 °C/min) of polyethers based on MBPE and 1,7-dibromoheptane (MBPE-7), MBPE and 1,11-dibromononane (MBPE-11), and corresponding copolyethers [MBPE-7/11(A/B)].

the isotropic–nematic and nematic–smectic mesophases to be observed in MBPE-7/11(80/20). All the other copolymers exhibit on cooling both the isotropic–nematic and nematic–smectic mesophases and no crystallization (Figure 9b). These thermal transitions are plotted as previously discussed in Figure 10a and extrapolation to MBPE-7 and MBPE-11 leads to the virtual isotropic–nematic and nematic–smectic mesophases reported in Table II. The analysis of the thermotropic parameters is shown in Figure 10b and the virtual enthalpic changes are reported in Table II. When the thermal transitions from the heating scans are analyzed as previously described (Figures 10), they reveal that MBPE-7/11 (40/60 to 60/40) copolymers exhibit both smectic and nematic enantiotropic mesophases. The extrapolation of these transitions and of the corre-

Table VI
Characterization of Polyethers Based on MBPE and 1,7-Dibromoheptane (MBPE-7) and 1,11-Dibromoundecane (MBPE-11) and of Corresponding Copolyethers [MBPE-7/11(*A*/*B*)]

copolymer MBPE-7/11(*A*/*B*) 7/11 mol ratio	$\bar{M}_n$	$\bar{M}_w/\bar{M}_n$	thermal transitions, °C, and the corresponding enthalpy changes (kcal/mru) in parentheses: heating	cooling
100/0	22100	1.76	g 7 k 85 (2.18) i	i 66 (2.01) k 0 g
80/20	34500	1.87	g 10 k 62 (0.13) k 79 (1.72) i	i 68 (0.87) n 60 (0.15) s 5 g
60/40	35100	1.86	g 10 s 69 (0.12) n 80 (0.87) i	i 69 (0.87) n 61 (0.07) s 2 g
50/50	29100	1.87	g 10 s 67 (0.13) n 77 (0.90) i	i 67 (0.94) n 59 (0.11) s 2 g
40/60	34000	2.13	g 11 k 50 (0.09) s 69 (0.09) n 80 (1.06) i	i 71 (1.02) n 63 (0.13) s 4 g
20/80	33500	1.89	g 13 k 49 (0.14) k 91 (3.30) i	i 72 (1.16) n 64 (0.15) s 34 (0.37) k 6 g
0/100	28500	2.02	g 5 k 101 (5.21) i	i 72 (1.09) n 64 (2.66) k

Table VII
Characterization of Polyethers Based on MBPE and 1,9-Dibromononane (MBPE-9) and 1,11-Dibromoundecane (MBPE-11) and of Corresponding Copolyethers [MBPE-9/11(*A*/*B*)]

copolymer MBPE-9/11(*A*/*B*) 9/11 mol ratio	$\bar{M}_n$	$\bar{M}_w/\bar{M}_n$	thermal transitions, °C, and the corresponding enthalpy changes (kcal/mru) in parentheses: heating	cooling
100/0	20600	1.38	g 6 k 75 k 80 k 91 (4.02) i	i 69 (1.05) n 58 (0.06) s 48 (2.13) k 0 g
80/20	33800	1.75	g 10 k 47 (0.30) k 77 k 86 (2.80[a]) i	i 72 (1.12) n 63 (0.15) s 19 (0.12) k 3 g
60/40	19700	1.63	g 10 k 45 (0.59) k 62 s 68 n 79 (1.08) i	i 70 (1.12) n 62 (0.14) s 19 (0.10) k 3 g
50/50	26800	1.86	g 12 k 47 (0.62) k 65 s 71 s 75 n 82 (1.08) i	i 71 (1.17) n 64 (0.08) s 22 (0.24) k 4 g
40/60	33600	1.75	g 13 k 50 (0.77) k 68 k 77 n 82 (1.94[a]) i	i 72 (1.22) n 65 (0.11) s 26 (0.35) k 6 g
20/80	21900	1.72	g 11 k 52 (0.16) k 72 k 81 k 89 (3.19[a]) i	i 71 (1.25) n 63 (0.10) s 41 (1.11) k 5 g
0/100	28500	2.02	g 5 k 101 (5.21) i	i 72 (1.09) n 64 (2.66) k

[a] Overlapping transitions.

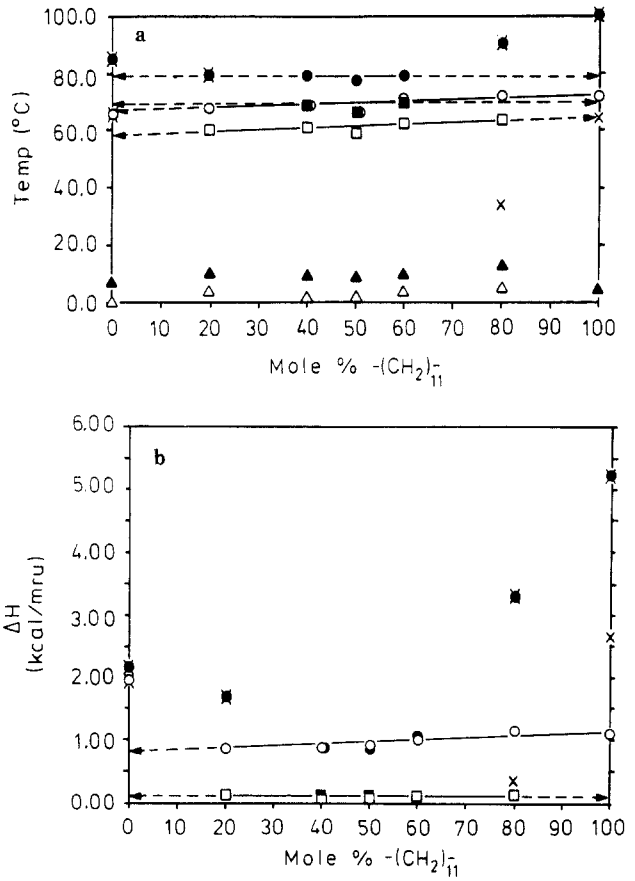

Figure 10. (a) Thermal transitions for homopolymers (MBPE-7 and MBPE-11) and copolymers [MBPE-7/11(*A*/*B*)]: (●) T_{ni}; (○) T_{in}; (◙) T_{ki}; (○) T_{ik}; (■) T_{sn}; (□) T_{ns}; (×) T_{nk} or T_{sk}; (▲) T_g(heating); (△) T_g(cooling). Arrows point to virtual transitions for the homopolymers. (b) Enthalpy changes for homopolymers (MBPE-7 and MBPE-11) and copolymers [MBPE-7/11(*A*/*B*)]: (●) ΔH_{ni}; (○) ΔH_{in}; (◙) ΔH_{ki}; (○) ΔH_{ik}; (■) ΔH_{sn}; (□) ΔH_{ns}; (×) ΔH_{nk} or ΔH_{sk}. Arrows point to enthalpies of virtual transitions for the homopolymers.

sponding enthalpies leads to the calculation of the nematic–isotropic and smectic–nematic virtual transitions and their corresponding enthalpy changes for MBPE-7 and MBPE-11 (Table II).

Last but not least, the copolymer system MBPE-9/11 (Figure 11) resembles in some ways the copolymer system MBPE-5/11, since MBPE-9 exhibits both a nematic and a smectic monotropic mesophase, while MBPE-11 only a nematic monotropic mesophase. The major difference is the fact that both MBPE-9 and MBPE-11 present a crystallization exotherm on cooling (Figure 11b) while MBPE-5 does not (Figure 3b). Heating and cooling DSC thermograms for MBPE-9/11 are presented in Figure 11 and the corresponding quantitative data are tabulated in Table VII. This is the first copolymer system whose crystallization is only depressed by copolymerization and at the same time this crystallization is preserved for the entire range of copolymer compositions (Figure 11b). The insertion of 20 mol % short spacer into this copolymer [MBPE-9/11(20/80)] depresses the crystallization temperature below the nematic–smectic mesophase. The nematic–smectic mesophase could not be observed in the parent MBPE-11 homopolymer. Thermal transitions from Figure 11b are plotted in Figure 12a and their corresponding enthalpies in Figure 12b. The extrapolation of the nematic–smectic linear dependence versus composition to MBPE-11 leads to its virtual nematic–smectic transition temperature (Figure 12a). Similarly, the extrapolation of the enthalpy change associated with this nematic–smectic transition (Figure 12b) leads to the virtual nematic–smectic enthalpy change of MBPE-11 (Table II).

The heating scans of the DSC traces for MBPE-9/11 copolymers are more complicated than of the previous sets of copolymers and require additional work for a complete understanding. Most of the MBPE-9/11 copolymers exhibit a crystallization exotherm on the heating DSC curves (Figure 11a) which seems to represent the continuation of the crystallization process from the cooling scans (Figure 11b). This crystallization exotherm is followed by a melting endotherm of very low enthalpy change (about 0.3–0.7 kcal/mru). The temperature of this melting endotherm is in contrast to other melting processes in that it is "composition independent". It might be associated

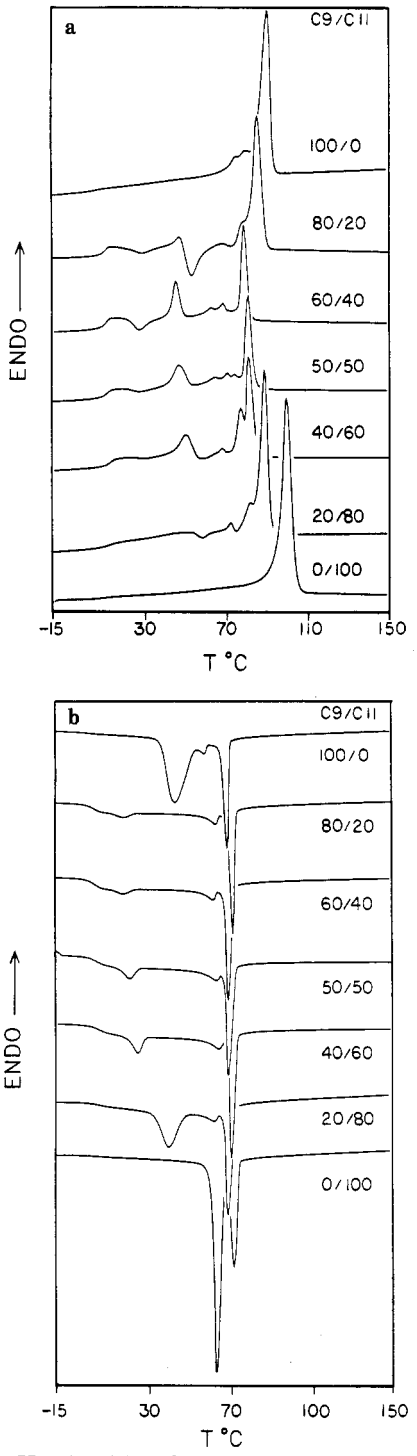

Figure 11. Heating (a) and cooling (b) DSC thermograms (20 °C/min) of polyethers based on MBPE and 1,9-dibromononane (MBPE-9), MBPE and 1,11-dibromononane (MBPE-11), and corresponding copolyethers [MBPE-9/11(*A*/*B*)].

with the self-organization of the long flexible spacer in a mesomorphic state of order between that of the "rotator" phase characteristic of polyethylene and the melt, i.e., possibly similar to that found in the "gel-phase" in lipids.[19] Related polymers containing shorter spacers than 11 methylene units do not reveal this kind of order.[19] However, additional work is required to confirm that this assumption is valid also for the present set of polymers. Above this endotherm there are a number of additional endotherms which are difficult to assign at this time. The last endotherm from the heating DSC curves relates to either a melting or a nematic–isotropic transition temperature. This last transition is plotted in the upper part

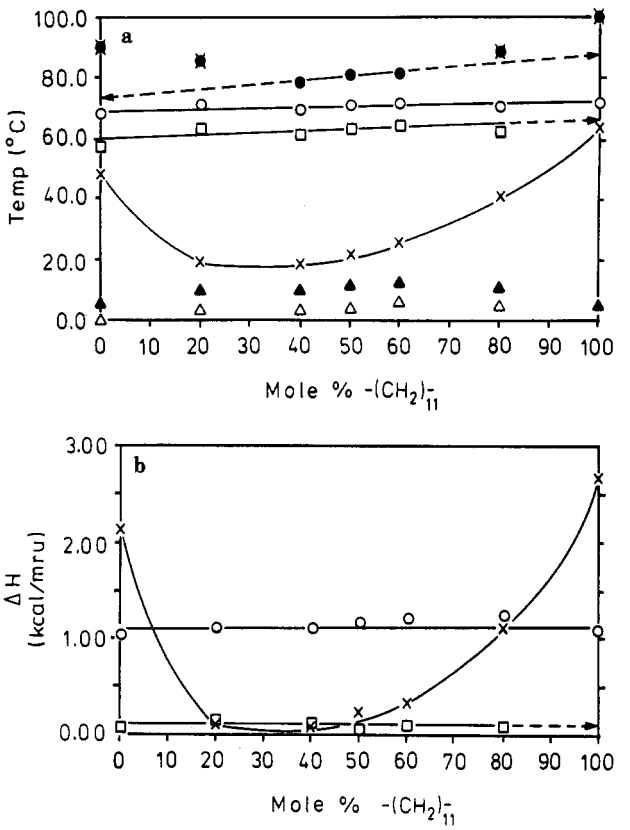

Figure 12. (a) Thermal transitions for homopolymers (MBPE-9 and MBPE-11) and copolymers [MBPE-9/11(*A*/*B*)]: (●) T_{ni}; (○) T_{in}; (■) T_{ki}; (□) T_{ns}; (×) T_{sk} or T_{nk}; (▲) T_g(heating); (△) T_g(cooling). Arrows point to virtual transitions for the homopolymers. (b) Enthalpy changes for homopolymers (MBPE-8 and MBPE-11) and copolymers [MBPE-9/11(*A*/*B*)]: (○) ΔH_{in}; (□) ΔH_{ns}; (×) ΔH_{nk} or ΔH_{sk}. Arrows point to enthalpies of virtual transitions.

of Figure 12a. Copolymers MBPE-9/11(60/40 to 40/60) exhibit nematic–isotropic transitions, while the other copolymers display crystalline–isotropic meltings. Extrapolation of the nematic–isotropic transition temperatures allowed the calculation of the virtual nematic–isotropic transition temperatures for both homopolymers (MBPE-9 and MBPE-11) as well as for the copolymers MBPE-9/11 (20/80 and 80/20) (Table II).

Figure 13a presents a threaded nematic texture which is characteristic of the nematic mesophases of all the polymers and copolymers discussed in this paper. In the case of the homopolymers, the transition from nematic to smectic is each time accompanied by the solidification of the polymer sample due to almost simultaneous crystallization. However, in the case of the copolymers, upon cooling into the temperature region of the smectic phase, the threaded texture becomes broken and a fan-shaped texture seems to be superimposed on it. A representative example of such a texture is shown in Figure 13b.

Finally Table VIII summarizes all the thermal tansitions exhibited by MBPE-X homopolymers, including the average data for the virtual thermal transitions and their corresponding enthalpy changes as obtained from the different sets of copolymers reported in Table II. Comparison of the virtual average transitions from Table VIII with the virtual transitions obtained from each set of copolymers (Table II) in part demonstrates a very good agreement.

The first conclusion of the experiments described in this paper is that flexible rodlike mesogenic units or rodlike mesogenic units based on conformational isomerism can be used in the synthesis of liquid crystalline polyethers even when separated by long flexible spacers. These series

Table VIII
Characterization of Averaged Virtual Liquid Crystalline Transitions and Their Corresponding Enthalpy Changes of the Homopolyethers (MBPE-*X*)

polymer	DSC scan	thermal transitions, °C, and the corresponding enthalpy changes (kcal/mru) in parentheses[a]
MBPE-5	heating	g 20 s [44 ± 2 (0.14 ± 0.02)] n [60 ± 4 (0.43 ± 0.10)] k 79 (1.44) k 115 (0.33) i
	cooling	i 51 (0.57) n 37 (0.10) s 13 g
MBPE-7	heating	g 7 s [64 ± 4 (0.15 ± 0.04)] n [76 ± 4 (0.59 ± 0.12)] k 85 (2.18) i
	cooling	i 66 (2.01) k [65 ± 1 (0.76 ± 0.04)] n [57 ± 2 (0.16 ● 0.05)] s 0 g
MBPE-9	heating	g 6 s [71 ± 1 (0.14)] n [80 ± 7 (0.99 ± 0.10)] k 75 k 80 k 91 (4.02) i
	cooling	i 69 (1.05) n 58 (0.06) s 48 (2.13) k 0 g
MBPE-11	heating	g 5 s [72 ± 3 (0.05 ± 0.01)] n [84 ± 5 (1.39 ± 0.04)] k 101 (5.21) i
	cooling	i 72 (1.09) n [66 ± 3 (0.11 ± 0.03)] s 64 (2.66) k

[a] [ ] averaged virtual transition temperatures and enthalpy changes.

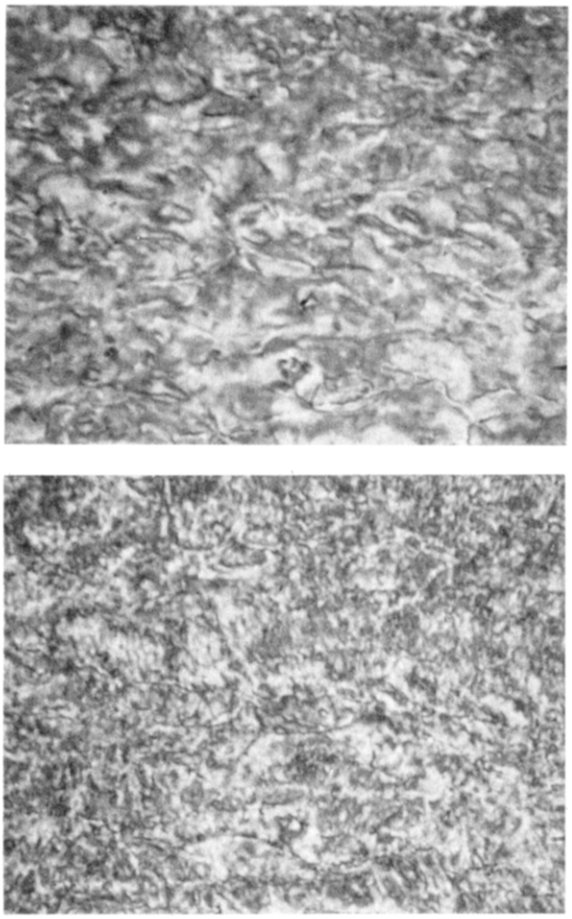

Figure 13. (a, Top) Threaded nematic texture exhibited by MBPE-7/9(50/50) copolymer after cooling to 72.1 °C from the isotropic state and annealing overnight (magnification 130×). (b, Bottom) Smectic texture exhibited by MBPE-7/9(50/50) copolymer after cooling from the nematic state to 55.1 °C and annealing for 30 min (magnification 130×).

of experiments have demonstrated that the synthesis of liquid crystalline polymers does not require the use of rigid, rodlike mesogenic units. These results are important since they open a new synthetic strategy based on novel structural requirements and thus enlarge the preparative arsenal available for the synthesis of liquid crystalline polymers. However, a number of previously unconsidered subjects of research have appeared simultaneously. The simplest topic involves the influence of a mesomorphic phase on the dynamic equilibrium between different conformational isomers of these "flexible" rodlike mesogenic units. This represents a fundamental problem of physical chemistry, since it has been predicted that when rodlike or linear conformations are in dynamic equilibrium with random-coil conformations, the rodlike conformation is preferred in the nematic phase.[20-22]

The second conclusion obtained from the experiments described in this paper seems to provide a definitive answer to one of the nonelucidated problems of semiflexible main-chain liquid crystalline copolymers. It refers to the influence of copolymer composition on mesomorphic phase transitions.[23] This conclusion is strongly supported by experimental results obtained recently in different laboratories.[9,14-18] It demonstrates that within the range of molecular weights where phase transitions are not affected by the nature of the polymer chain ends and are molecular weight independent, the liquid crystalline transitions of copolymers and their thermodynamic parameters should represent weight-averaged values of the transition temperatures and of the thermodynamic parameters of the parent homopolymers. Last but not least, as a consequence of this last conclusion and as repeatedly demonstrated in this paper, copolymerization becomes one of the most valuable tools for identification of mesophases in liquid crystalline polymers and copolymers.

All the polymers and copolymers described in this paper present a dynamic composition and, therefore, exhibit dynamic phase transitions. A complete characterization of these systems under different thermal conditions and the behavior of the polyethers and copolyethers containing an even number of methylene units in the flexible spacer will represent the subject of further publications from this laboratory.

Acknowledgment. Financial support of this work by the National Science Foundation, Polymers Program (DMR-86-19724), is gratefully acknowledged.

Registry No. MBPE, 115529-44-7; MBPE-5, 115529-45-8; MBPE-5/7, 115529-49-2; MBPE-5/9, 117068-59-4; MBPE-5/11, 117068-60-7; MBPE-7, 115529-46-9; MBPE-7/9, 117068-61-8; MBPE-7/11, 117068-62-9; MBPE-9, 115529-47-0; MBPE-9/11, 117068-63-0; MBPE-11, 115529-48-1; 3-methylanisole, 100-84-5; *m*-cresol, 108-39-4; 1-(2-methyl-4-methoxyphenyl)-2-(4-methoxyphenyl)ethanone, 93651-96-8; 4-methoxyphenylacetic acid, 104-01-8; (4-methoxyphenyl)acetyl chloride, 4693-91-8; 1-(4-methoxyphenyl)-2-(2-methyl-4-methoxyphenyl)ethane, 117068-58-3.

References and Notes

(1) Percec, V.; Yourd, R. *Macromolecules*, in press.
(2) Percec, V.; Pugh, C. In *Side Chain Liquid Crystal Polymers*; McArdle, C. B., Ed.; Blackie and Sons, Ltd.; Glasgow, in press.
(3) Hsu, C. S.; Percec, V. *J. Polym. Sci., Polym. Chem. Ed.* **1987**, *25*, 2909.
(4) Percec, V.; Rodriguez-Parada. J. M.; Ericsson, C. *Polym. Bull.* **1987**, *17*, 347.
(5) Hsu, C. S.; Percec, V. *J. Polym. Sci., Polym. Chem. Ed.*, in press.
(6) Nystrom, R. F.; Berger, C. R. *J. Am. Chem. Soc.* **1958**, *80*, 2896.
(7) Albrecht, W. L.; Gustafson, D. H.; Horgan, S. W. *J. Org. Chem.* **1972**, *37*, 3355.
(8) McOmie, J. F. W.; Watts, M. L.; West, D. E. *Tetrahedron* **1968**, *24*, 2289.
(9) Percec, V.; Nava, H. *J. Polym. Sci., Polym. Chem. Ed.* **1987**, *25*, 405.

(10) Percec, V.; Nava, H.; Jonsson, H. *J. Polym. Sci., Polym. Chem. Ed.* **1987**, *25*, 1943.
(11) Demus, D.; Richter, L. *Textures of Liquid Crystals*; Verlag Chemie: Weinheim, 1978.
(12) Shaffer, T. D.; Percec, V. *Makromol. Chem., Rapid Commun.* **1985**, *6*, 97.
(13) Feijoo, J. L.; Ungar, G.; Owen, A. J.; Keller, A.; Percec, V. *Mol. Cryst. Liq. Cryst.* **1988**, *155*(B), 487.
(14) Blumstein, A.; Vilagar, S.; Ponrathnam, S.; Clough, S. B.; Blumstein, R. *J. Polym. Sci., Polym. Phys. Ed.* **1982**, *20*, 877.
(15) Roviello, A.; Santagata, S.; Sirigu, A. *Makromol. Chem., Rapid Commun.* **1984**, *5*, 209.
(16) Watanabe, J.; Krigbaum, W. R. *Macromolecules* **1984**, *17*, 2288.
(17) Amendola, E.; Carfagna, C.; Roviello, A.; Santagata, S.; Sirigu, A. *Makromol. Chem., Rapid. Commun.* **1987**, *8*, 109.
(18) Fradet, A.; Heitz, W. *Makromol. Chem.* **1987**, *188*, 1233.
(19) Ungar, G.; Keller, A. *Mol. Cryst. Liq. Cryst.* **1988**, *155*(B), 313.
(20) Pincus, P.; de Gennes, P.-G. *Polym. Prepr. (Am. Chem. Soc., Div. Polym. Chem.)* **1977**, *18*, 61.
(21) Kim, Y. H.; Pincus, P. *Biopolymers* **1979**, *18*, 2315.
(22) Matheson, R. R.; Flory, P. J. *J. Phys. Chem.* **1984**, *88*, 6606.
(23) Ober, C. K.; Jin, J.; Lenz, R. W. *Adv. Polym. Sci.* **1984**, *59*, 130.

Copolymers of Styrene and Methyl α-(Hydroxymethyl)acrylate: Reactivity Ratios, Physical Behavior, and Spectral Properties

Albert O. Kress, Lon J. Mathias,* and Gustavo Cei

Department of Polymer Science, University of Southern Mississippi, Hattiesburg, Mississippi 39406-0076. *Received April 8, 1988*

ABSTRACT: Compositions of copolymers prepared in low conversion by bulk polymerization of methyl α-(hydroxymethyl)acrylate (MHMA) and styrene were determined by UV and ^{1}H NMR spectroscopy. Copolymers were further characterized by IR, ^{13}C NMR, DSC, and TGA. Reactivity ratios for both MHMA and styrene, determined by the methods of Kelen–Tudos and Tidwell–Mortimer, were found to be about 0.33. Joint confidence limits determined for the various methods indicate that the more precise estimates are those of Kelen–Tudos and Tidwell–Mortimer even though the monomer reactivity ratios determined by the methods of Fineman–Ross, Joshi–Joshi, and YBR were of comparable value. Physical properties were intermediate between those of homopolymers although glass transitions were found to be sensitive to MHMA composition and thermal history. An intramolecular cyclization with concurrent loss of methanol involving adjacent or near-neighbor MHMA units is proposed to account for the thermal behavior. Copolymers with high MHMA composition demonstrate reduced solubility in chloroform.

Introduction

The accurate estimation of copolymer composition and the precise determination of monomer reactivity ratios (MRR) are of importance for tailoring copolymers with desired physicomechanical properties. Acrylic copolymers have achieved great importance in a number of industrial applications; hence a knowledge of copolymer composition is an important step in the evaluation of their utility and properties. We have elsewhere reported the synthesis, purification, characterization, and polymerization of MHMA.[1]

The simple copolymer equation derived by Alfrey and Mayo, eq 1, describes the ratio of the instantaneous rates of consumption of the monomers as a function of the instantaneous monomer feed ratio and two reactivity ratios, r_1 and r_2:[2,3]

$$\mathrm{d[A]/d[B]} = \mathrm{([A]/[B])[(}r_1\mathrm{[A]} + \mathrm{[B])/([A]} + r_2\mathrm{[B])]} = m_1/m_2 \quad (1)$$

where d[A]/d[B] is the ratio of the instantaneous rates of consumption of the monomers A and B (A = M_1 and B = M_2, $M_1/M_2 = x_0$) by chain propagation. d[A]/d[B] is approximated at low conversions by the copolymer composition, $m_1/m_2 = y$, since d[A]/d[B] cannot be measured easily.

There are a number of difficulties in using eq 1 to determine MRR values. The ratio of instantaneous monomer consumption is only approximated by the copolymer composition; most copolymers show drift in the molar feed ratio. Linearized forms which use linear least squares are biased, and conversion is not generally considered.[4]

Integrated forms of eq 1 do not suffer from these same disadvantages. However, they require tedious and extensive computations and are not useful without a computer.[4-6,17]

Methods using the differential equation (eq 1) to determine MRR values are varied and generally fall into several broad catagories: linear,[7,8] intersection,[3,9,10] curve fitting,[11,12] computational,[13,14] and NMR triad evaluation.[15] There have been a number of reviews[6,16,17] and computer programs[18] published concerning the use and relative merits of a large number of methods.

A good determination of MRR values must meet five criteria as defined by Tidwell and Mortimer:[16] (1) It must give an unbiased estimate of the parameters. (2) It should utilize all the information resident in the data. (3) MRR values should not depend on reindexing or other arbitrary factors. (4) It should give valid estimates of the errors involved. (5) It should be relatively easy to use. The only approach that fits these conditions is a nonlinear least-squares method such as that described by Tidwell and Mortimer.

The Q–e scheme is an attempt to quantify monomer reactivity by considerations of inherent resonance (Q) and polar (e) factors of the adduct radical; steric factors, however, are not considered.[19] Once determined experimentally, MRR values can be employed in the Q–e scheme to predict copolymer composition in copolymerizations with other monomers.

Experimental Section

MHMA was readily prepared from methyl acrylate and paraformaldehyde in the presence of catalytic amounts of 1,4-diazabicyclo[2.2.2]octane (DABCO) as previously described.[1] **WARNING**: Small amounts of a potent byproduct generated by this method cause severe contact dermatitis. Other esters have not shown this deleterious behavior. Styrene was purified by

0024-9297/89/2222-0537$01.50/0